Journal of Fluorescence, Vol. 14, No. 6, November 2004 (©2004)

Utility and Considerations of Donor–Donor Energy Migration as a Fluorescence Method for Exploring Protein Structure-Function

Stanislav Kalinin[1] and Lennart B.-Å. Johansson[1,2]

Received June 2, 2004; accepted July 7, 2004

This review aims at surveying the use of electronic energy transport between chemically identical fluorophores (i.e. donors) in studies of various protein systems. Applications of intra- and interprotein energy migration are presented that make use of polarised steady-state and time-resolved fluorescence spectroscopic techniques. The donor-donor energy migration (DDEM) and the partial donor-donor energy migration (PDDEM) models for calculating distances between donor groups are exposed together with the most recent development of an extended Förster theory (EFT). Synthetic fluorescence depolarisation data that mimic time-correlated single photon counting experiments were generated using the EFT, and then further re-analysed by the different models. The results obtained were compared with the known parameters used to generate EFT data. Aspects on how to adopt the EFT in the analyses of time-correlated single photon counting experiments are also presented, as well as future aspects on using energy migration for examining protein structure.

KEY WORDS: Homotransfer; partial donor-donor energy migration; time-resolved fluorescence anisotropy.

INTRODUCTION

Numerous studies in molecular biology and biochemistry rely on different physical methods for obtaining structural information about macromolecules, such as proteins and nucleic acids. Powerful tools for determining the three-dimensional structure include the traditional methods of X-ray diffraction and multi-dimensional NMR-spectroscopy. While the former method relies on the preparation of crystals of high quality, NMR may, for larger molecules, suffer in spectral resolution, e.g. proteins with molecular masses exceeding about 200 amino acids. Furthermore NMR is a rather insensitive method that typically requires protein concentrations in the millimolar range. Unfortunately these concentrations are frequently associated with an unwanted protein aggregation. Distances can also be obtained from studies of electronic energy transfer between extrinsic or intrinsic chromophoric groups localised within macromolecules. The measurable distances that can be explored provide an important distinction between the traditional methods as well as the use of electronic energy transfer. While the X-ray and NMR methods measure short distances, typically those between nearest neighbouring atoms, the fluorescence methods provide longer distance values (10–100 Å), which are typically comparable to the size of proteins.

[1] Department of Chemistry, Biophysical Chemistry, University of Umeå, S-901 87 Umeå, Sweden.

[2] To whom correspondence should be addressed. E-mail: lennart.johansson@chem.umu.se

ABBREVIATIONS: A, acceptor of electronic energy; BD, Brownian dynamics; D, donor of electronic energy; D_j, the j-th donor D_j; the rotational diffusion constant of j-th donor; $\mathbf{D}_j$, director frame for the j-th donor; DAET, donor–acceptor energy transfer; DDEM, donor–donor energy migration; EFT, extended Förster theory; EM, energy migration; FRET, fluorescence resonance energy transfer; **L**, laboratory frame; M_j, molecule fixed frame for the j-th donor; PDDEM, partial donor–donor energy migration; R, the distance between the donor groups; **R**, coordinate system fixed in a protein; S_j, 2nd rank order parameter of the j-th donor; TCSPC, time-correlated single-photon counting; τ, the fluorescence lifetime.

1053-0509/04/1100-0681/0 © 2004 Springer Science+Business Media, Inc.

The electronic energy transfer between a donor (D) and an acceptor (A) group, the so-called donor-acceptor energy transfer (DAET), can be used to determine distances in macromolecules. In the literature, this process is also referred to as fluorescence resonance energy transfer (FRET). Several researchers have used DAET/FRET. Surveys of many related and relevant papers are found in books describing fluorescence spectroscopy [1,2], as well as in textbooks specialised on energy transfer [3,4]. When using DAET with extrinsic probes a major practical difficulty is to achieve the specific attachment of one donor, and one acceptor group within the *same* macromolecule. By using two chemically identical fluorophores in the labelling procedure however, this problem is circumvented [5]. Ideally the rate of energy transfer between identical fluorophores is reversible, which means that the electronic energy is exchanged back and forth within a pair. It can also migrate among several fluorophores within an ensemble of donors. For this reason many scientists use the concept *energy migration* in order to distinguish it from DA processes which are irreversible. Energy migration among donor molecules (also referred to as homotransfer) has been studied [6–11] and reviewed for decades [2,3,12,13]. However, relatively few studies deal with energy migration within pairs of donors, and it is only within the last few years that applications on proteins have been performed in order to obtain intramolecular distances. In the following, the process of *d*onor-*d*onor *e*nergy *m*igration within a pair of identical fluorescent groups is referred to as DDEM.

Although the problem with specific labelling is solved, the use of DDEM introduces other practical problems and theoretical demands. As is frequently stated in papers and textbooks, only fluorescence depolarisation experiments can monitor the rate of DDEM. This is not necessarily true however, as is explained in the present review. Nevertheless, the analyses of fluorescence depolarisation experiments in terms of the energy migration rate are more complex, as compared to DAET-experiments. The key-problem is that the rates of energy migration and the reorienting motions of the fluorescent molecule both contribute to the measurement. Different researchers have considered this problem and come up with different models and theories; these are discussed below. Therefore it is not surprising that few DDEM-studies have been published as compared to those using DAET. The reasons are likely connected with experimental difficulties, as well as the difficulty in performing a solid analysis of DDEM data.

Several diseases as well as biological functions are connected with the aggregation of proteins. This motivates an increasing interest in exploring such structures. The Alzheimer's, Creutzfeldt-Jacob's and prion diseases are important examples. For some proteins a regular aggregation is intimately connected with particular biological functions. This is the case with the muscle protein actin, as well as tubulin, which forms microtubules. X-ray and NMR-methods exhibit the highest potential for exploring such structures at an atomic level. While the challenge of preparing crystals for X-ray diffraction experiments should be easier with aggregating proteins, NMR spectra of protein aggregates become much harder to resolve. Consequently, in the study of structure and function of regular protein aggregates, fluorescence DAET and DDEM experiments can be very useful.

The present paper aims at reviewing and analysing different approaches for determining distance information from DDEM-experiments. A survey of DDEM-applications on biomacromolecular systems, mainly proteins, is also presented.

INTRA- AND INTERMOLECULAR DISTANCES IN PROTEINS

Hitherto, few publications consider energy migration (EM) as a means for distance measurement between two chemically identical fluorophores localised in a protein molecule. One reason is the difficulty connected with the analyses of experimental data. Because fluorescence depolarisation experiments are usually the prerequisite for detecting the EM process, the separation of the reorientational motions from the EM process becomes very complex. Previously several models that aim at handling this complexity were published [14–19]. A comparative study of these models is presented below in the section "Models of DDEM." At the same time that these models have been used, more basic theoretical analyses of EM between two interacting and reorienting donors were published [15,20,21]. Today a complete theoretical description exists which relates experimental data to the simultaneous motions and energy migration within a donor-donor pair. This theory is referred to as the extended Förster's theory (EFT). The EFT involves stochastic functions that make its applicability less straightforward. Recent studies show, however, that the EFT is applicable in studies of model systems [20,21], and even more recent results demonstrate how to apply EFT to the analyses of DDEM-data obtained with proteins [22].

DDEM has been used to explore structure-function properties of the plasminogen activator inhibitors type 1 and 2, denoted PAI-1 and PAI-2. These proteins belong to the large and diverse family of serine proteinase inhibitors (serpins) that encompass a wide range of proteins, mostly proteinase inhibitors [23]. The DDEM method was utilized to examine structural aspects of a protein complex that forms between PAI-1 and a urokinase-type

plasminogen activator: uPA [24]. Recently, the localisation of the active loop of PAI-1, which is involved in forming the complex, was also examined by using DDEM [25].

Hamman *et al.* [17] estimated distances between subunits of dimeric ribosomal protein L7/L12. They created cysteine mutations of the protein that were labelled with a sulfhydryl specific fluorescein derivative. Fluorescence steady-state depolarisation studies were performed and further analysed by a steady-state model, which is described below (cf. Eq. 9). Distances were calculated and the dissociation constant of the dimer was determined from the depolarisation data.

Runnels and Scarlata [19,26] have proposed a model to analyse the fluorescence depolarisation caused by DDEM within protein aggregates. This model was applied for distance measurements on protein aggregates [13], and Santos *et al.* [27] have estimated the distance between the two Trp residues within a dimer formed by the fragment of HIV protein gp41.

Lillo *et al.* [18] studied the interaction between the anticancer drug Taxol and microtubules. From time-resolved anisotropy measurements on fluorescein-labelled Taxol analogues, the authors were able to calculate the distance between Taxol binding centres. The time-resolved depolarisation model used for this is briefly discussed in the section "Models of DDEM." The model includes the depolarisation due to several fluorophores, which are arranged in a ring to represent one turn of helical structure of microtubule.

In some studies the contributions from the rotational motions might be negligible on the timescale of energy migration, and therefore one could assume that the fluorescence anisotropy only depends on the migration rate. This turned out to be a good approximation in studies of energy migration between flavins in lipoamide dehydrogenase [28]. For the analyses of data, the equations described by Tanaka and Mataga [29] or by Hochstrasser and co-workers [30] were applicable. In the particular case where the fluorescence depolarisation is solely due to energy migration, these two equations, as well as the DDEM model (Eq. (3)) coalesce into the following expression

$$r(t) = \frac{1}{5}[1 + S_\delta + (1 - S_\delta)\exp(-2\omega t)] \qquad (1)$$

In Eq. (1), the rate of energy migration is denoted ω, and $S_\delta = \frac{1}{2}(3\cos^2\delta - 1)$ where the angle δ is between the electronic transition dipoles of the interacting donors. This approximation is of particular interest for the case of EM between the chromophores of green fluorescent proteins (GFP) [31–34]. The Förster radius for GFP-GFP energy migration is about 47 Å [32,35]. Recently, Gautier *et al.* [32,36] observed EM between GFP chromophores *in vivo* using fluorescence anisotropy decay microscopy. They studied the herpes simplex virus thymidine kinase fused to GFP, in living cells. The authors estimated the distance between the two GFP chromophores within dimers of thymidine kinase. Clayton *et al.* [33] have demonstrated the possibility of measuring the time-resolved anisotropy by using fluorescence anisotropy microscopy in the frequency domain. The latter technique was further applied to study the concentration depolarisation of enhanced GFP fluorescence in bacteria.

PROTEIN AGGREGATES

Proteins may form oligomeres but also very large aggregates, which constitute a regular structure. For instance, transthyretin forms tetramers and mutants of transthyretin can form large aggregates, which are associated with the human amyloid disease, *familial amyloidic polyneuropathy* [37,38]. A common feature of the amyloid diseases is that the protein aggregates form crystals, so called amyloid fibrils, which depending on the kind of disease, are found as protein deposits in different extracellular spaces of tissues, or in a few cases as intracellular inclusions.

To characterise monomer/dimer transitions in solution, several authors have utilised the influence of EM on the fluorescence depolarisation [26,34,39–41]. Using the additivity of the fluorescence anisotropy [1] calculation of the fraction of each state becomes possible, provided one knows what kind of aggregates are formed. In many cases, however, the fluorescence depolarisation data contain additional structural information.

Runnels and Scarlata [19,26] have modelled the fluorescence depolarisation due to fluorescence EM within protein aggregates. The model was applied to study the oligomerisation of melittin, which is well characterized and therefore provides a suitable test system. The N-terminal of melittin was then labelled with fluorescein isothiocyanate. The authors demonstrated that their model could be used to estimate the number of subunits in oligomers.

Blackman *et al.* [41] used a numerical Monte-Carlo approach to analyse the time-dependent fluorescence anisotropy of the erythrocyte anion exchange protein oligomers, band 3, labelled with eosin. They concluded that the dimeric and tetrameric band 3 could explain DDEM data, obtained with ghost membranes, without including any substantial clustered fraction of band 3.

Tubulin is another well-known protein that forms the building unit of microtubules (see e.g., [42]). Recently

Acuna and coworkers [18] have studied the interaction of the anticancer drug Taxol with microtubules, as is further described below in the section "Intra and Intermolecular Distances in Proteins."

Varma and Mayor [43] have demonstrated that glycosyl-phosphatidyl-inositol (GPI)-proteins anchored at the surface of living cells are organized in domains. They measured the extent of fluorescence depolarisation due to energy migration between GPI-anchored folate receptors, bound to a fluorescent analogue of folic acid. The fluorescence anisotropy was density-independent, which is not consistent with uniform random distribution at the cell surface. Rather, this would be expected for GPI-anchored proteins arranged in domains, so that the average distance between fluorophores is density-independent. In a similar way MacPhee *et al*. [44] studied the interaction of an α-helical peptide derived from apolipoprotein C-II with a model lipid surface. The peptide was labelled at the N-terminus with 7-nitrobenz-2-oxa-1,3-diazole (NBD). The efficiency of energy transfer between NBD groups was not consistent with a random distribution of peptides on the lipid surface, which indicates self-association of the lipid-bound peptides. A similar approach was also used in the characterisation of fluorescent lipid derivatives, to distinguish between a random distribution on the lipid surface and aggregation of the probes. (see e.g. Prieto *et al*. [45]).

Donor-donor systems could also be used for quantitative investigation of the distribution of peptides or proteins in lipid bilayers. It might then be interesting to reveal whether peptides/proteins attract each other or actually form aggregates, or are randomly distributed as monomers in the lipid bilayers. From the analyses of fluorescence depolarisation experiments performed with fluorophore-labelled proteins of different concentrations in the lipid bilayers, it is possible to obtain the surface concentration (C_{exp}) of labelled proteins, which is further compared to the theoretical value for a random distribution (C_{calc}). Values of $C_{exp} > C_{calc}$, strongly suggest that the molecules posses mutual affinity. Previously this idea was used to study the eventual aggregation of sulphatide lipids in mixtures with phospholipids [46], by applying theoretical models developed by Baumann and Fayer [11]. A feature of this approach was also used to examine the eventual aggregation of the membrane spanning hydrophobic α-helical peptide, WALP16 [47]. The peptides were labelled at the C-terminus with a polar fluorophore (rhodamine 101), and solubilised at different molar ratios into the bilayers of unilamellar lipid vesicles. Upon increasing the concentration of WALP16 in the lipid bilayers, the fluorescence anisotropy decreased, as is expected due to increasing EM. But at even higher peptide concentrations the fluorescence lifetime also started to decrease, which was consistent with the formation of rhodamine 101-dimers. Thereby the dimers acted as excitations traps, or acceptors of the monomeric rhodamine 101. By using previously developed models [11] in the data analyses, it was concluded that the transmembrane spanning peptide WALP16 exhibits an inherent affinity towards aggregation in lipid bilayers. Moreover, for certain lipid-WALP16 systems, the analyses of DAET data were only compatible with one-dimensional aggregation.

MODELS OF DDEM

According to Föster's famous theory of weak dipole-dipole coupling between an electronically excited chromophore and a second chromophore in its electronic ground state, the rate of energy migration ω is given by

$$\omega = \frac{3\langle\kappa^2\rangle}{2\tau}\left(\frac{R_0}{R}\right)^6 \tag{2}$$

Here τ, $\langle\kappa^2\rangle$, R and R_0 in Eq. (2) stand for the fluorescence lifetime of the donor, the averaged square of the angular part of the dipole-dipole interaction, the distance between the interacting molecules and the Förster radius, respectively. In the following we consider DDEM within a pair of chemically and photophysically identical fluorescent groups (denoted D_1 and D_2), which are covalently linked to a macromolecule, such as a protein. From depolarisation measurements the time-resolved fluorescence anisotropy is obtained for a coupled system (D_1D_2), as well as for the single donors: D_1 and D_2. These time-resolved anisotropies are denoted $r(t)$, $r_1(t)$ and $r_2(t)$, respectively. The corresponding steady-state anisotropies are r, r_1 and r_2, respectively. The anisotropy contribution to $r(t)$ from donors excited indirectly through the energy migration $D_1 \rightarrow D_2$ and $D_2 \rightarrow D_1$ are denoted by $r_{12}(t)$ and $r_{21}(t)$. In this section we present different models that were previously used for analysing time-resolved and steady-state fluorescence data. The models I–III and IV–VI refer to the analyses of time-resolved fluorescence and steady-state depolarisation data, respectively.

Model I

The DDEM model was developed for analysing the fluorescence anisotropy obtained from experiments with singly and doubly fluorophore-labelled proteins [5,14].

$$r(t) = \frac{1}{4}[r_1(t) + r_2(t)] \times [1 + \exp(-2\omega t)] + \frac{1}{4}[r_{12}(t) + r_{21}(t)] \times [1 - \exp(-2\omega t)]$$

$$r_j(t) = r_0\left[\left(1 - S_j^2\right)\gamma_j(t) + S_j^2\right] \quad j = 1, 2$$
$$r_{12}(t) = r_{21}(t)$$
$$= r_0\left[(\rho_0 - S_1 S_2 S_\delta) \times \frac{1}{2}(\gamma_1(t)) + \gamma_2(t)) + S_1 S_2 S_\delta\right] \tag{3}$$

In Eqs. (3) r_0 is the limiting anisotropy and S_j is a second rank order parameter for each of the two donor groups. The order parameter describes the orienting distribution of the transition dipoles, which is assumed to be effectively uniaxially symmetric about the z_{D_j}-axis ($j = 1, 2$) of a frame attached to the macromolecule (see Fig. 1). The angle between the z_{D_j}-axes is δ and $S_\delta = \frac{1}{2}(3\cos^2\delta - 1)$. The maximum contribution to the anisotropy from the secondary excited fluorophore is given by ρ_0, and $\gamma_j(t)$ describes the reorientation dynamics of the donor molecules. In the analyses of DDEM-data ω, ρ_0 and δ are fitting parameters.

Model II

Barcellona and Gratton [16] as well as Jameson and coworkers [17] have presented a model that slightly differs from Eqs. (3). By adapting Eqs. (5) in the reference [16] to the notation used for Model I one obtains:

$$F_\parallel(t) = \frac{F_0}{3}(1 + r_1(t) \times [1 + \exp(-\omega t)] + r_{12}(t) \times [1 - \exp(-\omega t)])\exp(-t/\tau)$$

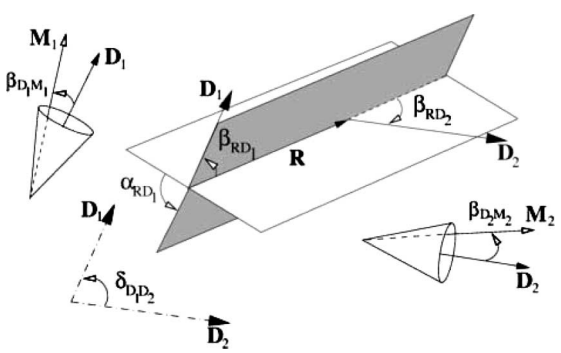

Fig. 1. The coordinate systems and angles needed for describing electronic energy migration within a donor pair. The electronic transition dipole moments of the donors (D_1 and D_2) are coinciding with the z-axis of the molecular frames $\mathbf{M}_1$ and $\mathbf{M}_2$. The donors are assumed to be uniaxially oriented about the z-axis of the director frames $\mathbf{D}_1$ and $\mathbf{D}_2$, which are attached to a rigid macromolecule. The concept configuration here means the orientation of $\mathbf{D}_1$ and $\mathbf{D}_2$ with respect to the $\mathbf{R}$-frame, which is defined by the three orienting angles (β_{RD_1}, α_{RD_1} and β_{RD_2}) because α_{RD_2} is taken to be 0. The z-axis of the $\mathbf{R}$-frame connects the centre of mass of D_1 and D_2 at the distance R.

$$F_\perp(t) = \frac{F_0}{3}\left(1 - \frac{r_1(t)}{2} \times [1 + \exp(-\omega t)] - \frac{r_{12}(t)}{2} \times [1 - \exp(-\omega t)]\right)\exp(-t/\tau) \tag{4}$$

In Eqs. (4) $F_\parallel(t)$ and $F_\perp(t)$ denote the time-resolved fluorescence intensities polarised parallel and perpendicular to the polarisation of the excitation light, respectively. F_0 is a constant. To simplify Eqs. (4), the authors [17] have assumed that $r_{12} = 0$. It then follows that

$$r(t) = \frac{1}{2}r_1(t) \times [1 + \exp(-\omega t)] \tag{5}$$

Model III

Recently Acuna and coworkers [18] have suggested modelling the fluorescence depolarisation as a product of all contributing factors (cf. Eq. (6) in ref. [18]). If the tumbling of a macromolecule is negligible on the fluorescence timescale, the anisotropy is given by

$$r(t) = r_1(t)\left[\left(1 - S_{\mathrm{ET}}^2\right)\exp(-2\omega t) + S_{\mathrm{ET}}^2\right] \tag{6}$$

Here S_{ET} is a second rank order parameter which is determined by assuming that energy transfer is the only contribution to the fluorescence depolarisation.

In addition to these models, EM was simulated by means of a Monte-Carlo algorithm. This numerical approach can be used in the analysis of energy migration within pairs of chromophores [41,48], in multichromophoric molecules [49], Langmuir-Blodgett films [50] and oriented polymer films [51], as well as in lipid membranes [52]. The reorienting motions of fluorescent molecules can also be taken into account [53,54].

Model IV

Different integrated versions of the models mentioned above, which are intended for analysing the fluorescence steady-state anisotropy, are given in the literature. For a pair of interacting fluorophores, Runnels and Scarlata [19] have suggested the following expression for the fluorescence anisotropy:

$$r = r_1\left(\frac{1 + \tau\omega}{1 + 2\tau\omega}\right) + r_{\mathrm{ET}}\left(\frac{\tau\omega}{1 + 2\tau\omega}\right) \tag{7}$$

By using Eq. (7) and assuming that $\langle\kappa^2\rangle = 2/3$ and $r_{\mathrm{ET}} = 0$ [19], the distance (R) between the interacting fluorescent groups can be calculated from

$$R = R_0\left(\frac{2r - r_1}{r_1 - r}\right)^{1/6} \tag{8}$$

Model V

Jameson and co-workers have proposed a formula that relates the efficiency of energy transfer to the anisotropies r and r_1 (cf. Eq. (3) in reference [17]). From that expression it follows that

$$R = R_0\left(\frac{1}{2} \times \frac{2r - r_1}{r_1 - r}\right)^{1/6} \tag{9}$$

Model VI

Provided $r_1(t) = r_2(t) = r_0 \exp(-t/\phi)$ and $r_{12}(t) = r_{21}(t) = 0$, the integration of Eq. (3) leads to an expression for calculating the distance according to

$$R = R_0\left(\frac{r_1}{r_0} \times \frac{2r - r_1}{r_1 - r}\right)^{1/6} \tag{10}$$

COMPARISON BETWEEN THE MODELS I–VI

In the following section we intend to compare the different DDEM-models by using them to re-analyse synthetic data that was generated using the extended Förster theory (EFT), being a complete theoretical description of EM within DD-pairs [15]. Because the EFT depends on stochastic functions due to the time-dependent reorientations of the interacting molecules, the EFT is not directly applicable. The reorientation, in terms of the orientational trajectories, can be handled by using Brownian dynamics simulations, as described elsewhere [20,21]. The orientational trajectories were generated by a recently developed method [55]. Two different uniaxial potentials were used in the simulations, namely a cone- and a Maier-Saupe potential.

The cone potential assumes that the rotational diffusion is free within a cone. Then, by representing the electronic transition dipole moment as a vector and describing its orientation by a polar angle β, the mathematical description of the cone potential is given by:

$$U(\beta) = \begin{cases} 0 & \beta \le \theta_c \\ \infty & \beta > \theta_c \end{cases} \tag{11}$$

Fluorescence depolarisation data was generated for all possible combinations of definite values chosen for the cone angle (θ_c), the rotational diffusion constant (D), and the angle (δ) between the symmetry axes of the D_1 and D_2 cone potentials (cf. Fig. 1). The following cone angles were used, $\theta_c = 30°$, $60°$ and $180°$ (i.e. free diffusion) corresponding to the order parameters $S \approx 0.808$, 0.375, and 0, respectively. The diffusion constants were chosen to be $D = 1/(2\tau)$, $1/(6\tau)$ and $1/(18\tau)$. The angle δ was chosen to be $0°$, $30°$, $60°$, and $90°$.

A physically more tractable potential is the Maier-Saupe potential [56], which in its most simple form reads:

$$U(\beta) = -\Phi \cos\beta \tag{12}$$

To obtain order parameters similar to those for $30°-$ and $60°-$ cones the values of Φ were taken to be 14.6 and 3.4 (in units of kT), respectively. The diffusion constants were chosen to be $D = 1/(2\tau)$, $1/(6)$ and $1/(18\tau)$. The angle δ was chosen to be $0°$, $30°$, $60°$, and $90°$.

The generated fluorescence depolarisation data thereby represents the fluorescence anisotropy of single donors $\{r_1(t)\}$ that undergo anisotropic reorientations in the absence of energy migration. For each set of parameters, 10^6 pairs of trajectories were generated. Each trajectory consisted of 1024 points and the time step was 0.05τ. If necessary, the time step was reduced so that the difference between the theoretical and the calculated order parameters was within ± 0.001. For the coupled system of donors, the time-dependent fluorescence anisotropy was generated using the EFT, as is described elsewhere [20,21].

The time-resolved depolarisation data was analysed by a least-square fitting of the models I–III to the generated fluorescence anisotropy decays. The steady-state fluorescence anisotropy corresponding to generated depolarisation data was calculated by integration. The models IV–VI were then used to analyse the data. The exact value of $\langle\kappa^2\rangle$, calculated from the order parameters and δ-angle, was then used in the analyses of the time-resolved data, while for all steady-state models (IV–VI), $\langle\kappa^2\rangle = 2/3$ was assumed. This means that it is usually not possible to estimate $\langle\kappa^2\rangle$ solely from steady-state experiments.

In many applications of these models, the donor-donor distance (R) is the most interesting parameter to determine. For this reason we have compared the values of the distances obtained using six models, with the correct value. The range of distances examined was from 0.6 R_0 to 1.7 R_0. Because the comparative study combines a wide range of parameters, a detailed presentation of all results becomes difficult. The most interesting aspect is to obtain distances. Therefore we present the percentage of cases for which the relative errors are within 5, 10 and 20% (see Fig. 2). A comparison of the models show that for large values of the order parameters (i.e. $S \approx 0.8$) and in particular, $\delta = 0°$, only Model I appears appropriate, while for systems of low order the Models I–III work equally well. For a system with high and low order parameters typical anisotropy decays are illustrated in Fig. 3. For the former case ($\theta_c = 30°$ and $\delta = 0°$, Figs. 3A and C) only the DDEM model fits very well with the generated data and

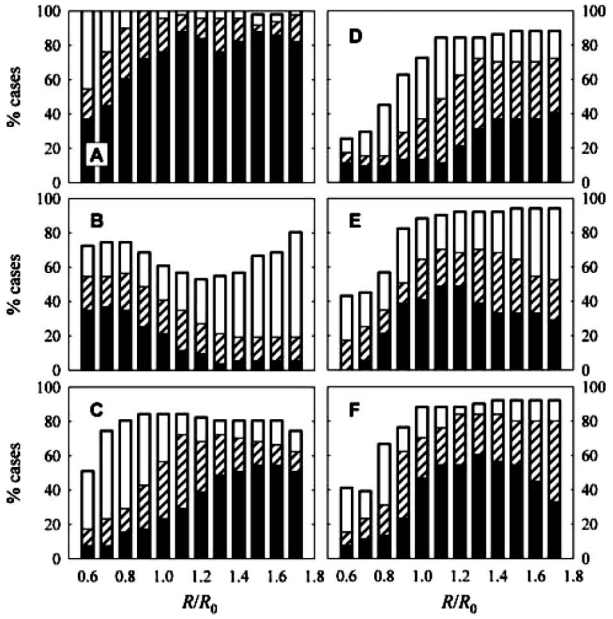

Fig. 2. The average errors in distance obtained using different models. Percentages of cases for which the relative error was within 5, 10 and 20% are shown as black, hatched and white bars, respectively. The data set is described in the text and was analysed using A: Model I, Eq. (3) [14]; B: Model II, Eq. (5) [16, 17]; C: Model III, Eq. (6) [18]. The steady-state models were also used, shown in D: Eq. (8) [19]; E: Eq. (9) [17]; and F: integrated DDEM model, Eq. (10). The errors in R are shown for different R/R_0 ratios.

the distance of 0.99 R_0. However, if the reorientations of the donors are unconstrained ($\theta_c = 180°$, Figs. 3B and D), all of the three models for time-resolved decays describe EM rather accurately. The errors of the distances obtained are within a few percent, as mentioned above. Model III works best for migration rates (ω), being much slower than the rotational correlation times (i.e. $1/(2\omega) >> \phi$), which is also suggested by Acuna and co-workers [18]. The distances calculated from the steady-state anisotropy using the Models IV–VI provide reasonable accuracy for low order and distances where $R \approx R_0$. The above conclusions are very similar for both the cone and the Maier-Saupe potential.

In some cases poissonian noise was added in order to mimic true TCSPC data [57]. The decay curves, $F_{\parallel}(t)$ and $F_{\perp}(t)$, were then constructed and re-analysed [58]. This procedure allows one to investigate both systematic and random deviations of the extracted parameters from the values assumed in simulations [59]. The average distances calculated from the mimicked TCSPC data, using models I–III, were close to the results obtained by analysing the data without adding noise. The random scatter of the extracted distances was noticeable for extreme values, typically when $R \leq 0.7R_0$ and $R \geq 1.5R_0$.

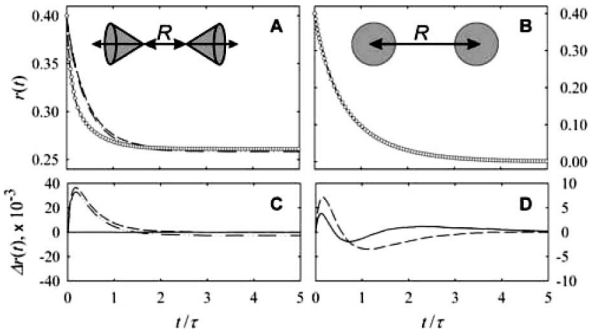

Fig. 3. Fluorescence depolarisation of pairs of fluorophores in the presence of energy migration, for A: a high order system, $\theta_c = 30°$, $\delta = 0°$, $D = 1/(6\tau)$, $R = R_0$, and for B: $\theta_c = 180°$, $D = 1/(6\tau)$, $R = R_0$. Best fits to the generated data (○) were obtained using the DDEM model (Model I, ——), the model II (- - -), and the model III suggested by Acuna *et al.* [18] (— · · — · · —). The differences between the generated data and the best fits are shown in plots C and D for the high and low order systems, respectively (some curves are almost indistinguishable from each other). The Models I, II, and III applied to fit the generated data, which are shown in plot A, yield the distances 0.99 R_0, 0.49 R_0, and 0.29 R_0, respectively. The corresponding obtained distances for the low-ordered system (plot B) are 1.02 R_0, 0.96 R_0, and 1.02R_0, respectively.

PARTIAL DONOR–DONOR ENERGY MIGRATION

A drawback with the DDEM method is the need to use fluorescent groups that exhibit very similar photophysics, irrespective of their localisation in a protein structure. Most fluorescent molecules do not fulfil this criterion, which strongly limits the number of useful probes. It is, however, still possible to make use of the interaction between two chemically identical but *photophysically non-identical* D-molecules. The EM within such a DD-pair will influence the photophysics observed, and it becomes possible to deduce how the fluorescence relaxation depends on the rate of EM [60]. It means that fluorescence lifetime measurements could be used for determining distances. Thus, both the fluorescence lifetime and depolarisation experiments contain distance information. To distinguish from DDEM and DAET, we refer to this case as being *p*artial *d*onor-*d*onor *e*nergy *m*igration (PDDEM), because here one deals with DD-pairs for which the energy migration is only partially reversible. Strictly speaking, PPDEM can occur in any DD-pair, for which each D in the absence of EM exhibits non-exponential photophysics. This is true even if the two D-molecules have identical non-exponential decays. The theoretical treatment of PDDEM is an extension of a previously developed model of partly reversible DAET [61]. The PPDEM-method can be considered as the most general treatment of electronic energy transfer between two chemically identical fluorophores,

which, as the photophysics becomes very similar leads to the DDEM-method. Therefore the case of PDDEM is also useful for extracting distances, as is shown below.

The PDDEM-process may explain the shortening of the fluorescein lifetimes in melittin aggregates reported by Runnels and Scarlata [19]. The process may also explain the fluorescence lifetimes and quantum yields observed for tryptophan residues in proteins [62–64]. In the latter papers Engelborghs has shown that the PDDEM process can explain changes in fluorescence lifetimes [63] and quantum yields [64] of Trp residues the PAI-1 and Barnase.

To accurately determine distance between two D-groups from fluorescence lifetime measurements, a significant difference between their lifetimes is needed [60]. Typically, the (average) lifetimes should differ in a ratio of 2:3. For small differences one could use a corrected form of the expression for the DDEM-anisotrophy [60,65]. For D-groups covalently bonded to a protein, however, one could increase this difference by adding quenchers whose efficiency of quenching likely depends on the donor location in a protein structure. Recently this idea was tested by using iodide as a quencher of BODIPY-groups that were specifically bound to cysteines in PAI-2 [65]. The structures of PAI-2 and the sulfhydryl-specific BODIPY derivative (SBDY) are shown in Fig. 4. The PDDEM approach has also been used to analyse EM between ionic forms of xanthene dyes [66,67].

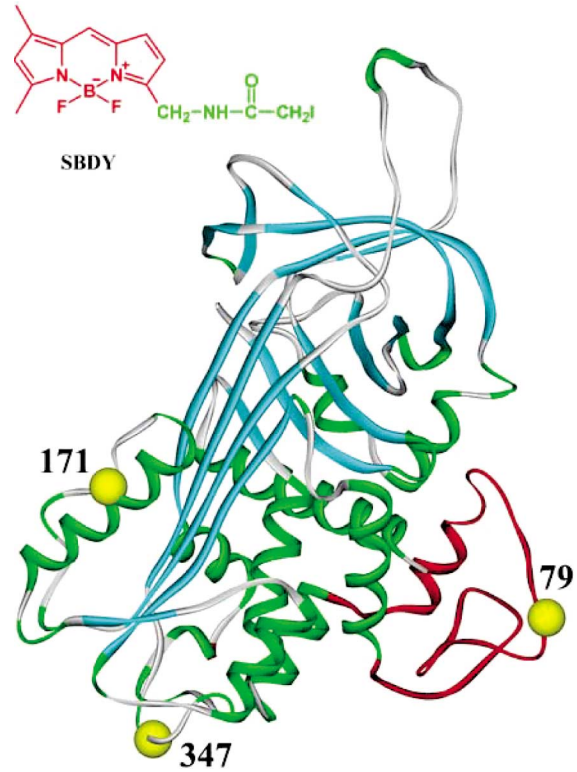

Fig. 4. The ribbon structure of plasminogen activator inhibitor type 2 (PAI-2) in which the CD-loop is shown in red. The yellow spheres indicate C_α-atoms of the Cys residues that were labelled with SBDY {*N*-(4,4-difluoro-5,7-dimethyl-4-bora-3a,4a-diaza-*s*-indacene-3-yl) methyl iodoacetamide}. The chemical structure of SBDY is also shown.

EFT AND PERSPECTIVES

Hitherto the information content of the EM-process within D-pairs was mainly used in a qualitative manner, for instance to indicate the aggregation of proteins. The models available for obtaining distance information from depolarisation experiments are based on approximations, which under certain conditions are not fulfilled. The main question concerns the angular dependence and dynamics of κ^2 in Eq. (2). Today it should be possible to leave all these models and instead use the EFT, which constitutes a full description of the excitation probabilities, as well as the fluorescence anisotropy. The fluorescence anisotropy is given by

$$r(t) = \frac{r_0}{2}[\rho_1(t) + \rho_2(t) + \rho_{12}(t) + \rho_{21}(t)] \qquad (13)$$

The probability of initial excitation is equal for D_1 and D_2 and the corresponding time-dependence is $\chi(t)$. The anisotropy constitutes the following contributions:

$$\rho_i(t) = \langle P_2[\hat{\mu}_i(0) \cdot \hat{\mu}_i(t)]\chi(t)\rangle \quad i = 1, 2 \qquad (14)$$

$$\rho_{ij}(t) = \left\langle P_2\left[\hat{\mu}_i^R(0) \cdot \hat{\mu}_j^R(t)\right](1 - \chi(t))\right\rangle, \quad i = 1, 2\,(i \neq j) \qquad (15)$$

In Eqs. (14) and (15) $\hat{\mu}$ denotes the unit vector of the transition dipole moment, and the superfix indicates an orientational transformation with respect to a coordinate system, fixed in the macromolecule (See Fig. 1). The equation describing the excitation probability of the initially excited donor group is expressed as a function of the rate of energy migration (ω) given by [15].

$$\chi(t) = \frac{1}{2}\left[1 + \exp\left(-2\langle\omega\rangle t - 2\int_O^t [\omega(t') - \langle\omega\rangle]\,dt'\right)\right]$$

$$\chi(0) = 1 \qquad (16a)$$

$$\langle\omega\rangle = \lim_{T\to\infty}\frac{1}{T}\int_O^T \omega(t')\,dt'$$

$$\omega(t') = \Lambda\kappa^2(t')$$

$$\Lambda = \frac{3}{2\tau}\left(\frac{R_0}{R}\right)^6$$

$$k(t') = \hat{\mu}_1^R(t') \cdot \hat{\mu}_2^R(t') - 3\left(\hat{\mu}_1^R(t') \cdot \hat{R}\right)\left(\hat{\mu}_2^R(t') \cdot \hat{R}\right) \tag{16b}$$

Eq. (16a) is the formal solution to the stochastic master equation, which was previously derived from the stochastic Liouville equation [15].

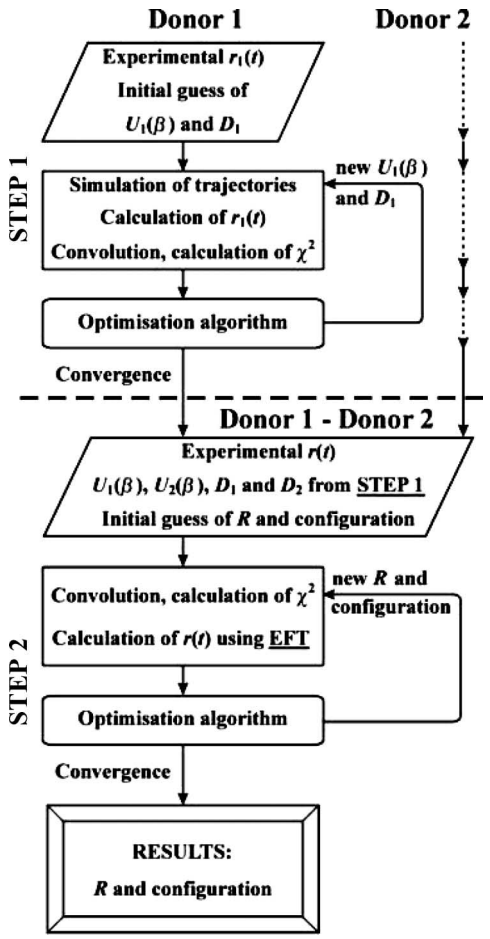

Fig. 5. Flow scheme of the simulation-deconvolution algorithm. At STEP 1, the fluorescence anisotropy of the two donors in absence of energy migration is analysed. Calculation starts with an initial guess of the potentials $U_1(\beta)$ and $U_2(\beta)$ and the diffusion coefficients D_1 and D_2 and BD-simulations of the trajectories for each donor. The time-resolved fluorescence anisotropies $r_1(t)$ and $r_2(t)$ calculated from these trajectories are compared with the experimental data, and the residuals are passed to the optimisation subroutine. The parameters of the potentials $U_1(\beta)$ and $U_2(\beta)$ as well as the values of D_1 and D_2 are then changed for each iteration until convergence is reached. At STEP 2 the depolarisation $r(t)$ of the coupled D_1D_2 system is analysed to obtain the distance R between D_1 and D_2 and the configuration of the system (angles β_{RD_1}, α_{RD_1}, and β_{RD_2} in Fig. 1). The theoretical $r(t)$ is calculated according to EFT and using $U_1(\beta)$, $U_2(\beta)$, D_1, and D_2 obtained at STEP 1. The result is compared with the experimental $r(t)$, R and configuration are changed accordingly by the optimisation algorithm. The procedure is repeated until convergence is reached.

A difficulty with the EFT in the analyses of TCSPC data is the lack of an explicit analytic expression that can be used in the deconvolution procedure. To handle the stochastic dependence one needs to use simulations methods, assuming e.g. Brownian diffusion (BD) in a cone potential. A schematic of the simulation-deconvolution approach is displayed in Fig. 5. To start, the local reorientations of the donors, described by potential functions $\{U_1(\beta)$ and $U_2(\beta)\}$ and diffusion constants (D_1 and D_2) are determined from the depolarisation of the donors D_1 and D_2 in the absence of EM (STEP 1 in Fig. 5). The time-resolved anisotropy of the D_1D_2 system is described by EFT (Eqs. (13)–(16)), which is fitted to the experimental data by varying coupling strength Λ and configuration of the donors, described by angles β_{RD_1}, α_{RD_1} and β_{RD_2}, as shown in Fig. 1. As a result of STEP 2, one obtains the distance between D_1 and D_2 and the configuration of the coupled system (Fig. 1, angles β_{RD_1}, α_{RD_1} and β_{RD_2}).

In addition to the complete theoretical description of EM, new methods for incorporating fluorescent probes into protein structures are under development. With comparison to standard methods of protein labelling [68], the site-specific incorporation of unnatural fluorescent amino acids into proteins is a very promising idea [69–74]. This approach could circumvent difficulties, such as: low labelling efficiency, perturbation of the protein structure, and the uncertainty in distance measurements due to significant linker lengths between the polypeptide backbone and a fluorescent group. Taken together, the EFT combined with methods that allows for flexibility in the labelling may become a versatile tool that complement standard NMR- and X-ray-techniques, where protein sizes, concentrations and crystalline qualities are inadequate.

ACKNOWLEDGMENTS

We are grateful to the Swedish Research Council and the Kempe Foundations for financial support.

REFERENCES

1. J. R. Lakowicz (1999). *Principles of Fluorescence Spectroscopy*, 2nd ed., Kluwer Academic/Plenum, New York.
2. B. Valeur (2002). *Molecular Fluorescence. Principles and Applications*, Wiley-VCH, Weinheim, Germany.
3. B. W. Van der Meer, G. Coker III, and S.-Y. S. Chen (1994). *Resonance Energy Transfer: Theory and Data*, VCH New York.
4. N. L. Vekshin (1997). *Energy Transfer in Macromolecules*, 1st ed., Spie Press, Bellingham, WA.
5. J. Karolin, M. Fa, M. Wilczynska, T. Ny, and L. B.-Å. Johansson (1998). Donor–Donor Energy Migration (DDEM) for determining

intramolecular distances in proteins: I. application of a model to the latent Plasminogen Activator Inhibitor-1 (PAI-1). *Biophys. J.* **74**, 11–21.
6. E. Gaviola and P. Pringsheim (1924). Einfluss der Konzentration auf die Polarisation der Fluoreszenz von Farbstofflosenungen. *Z. Physik* **24**, 24.
7. P. P. Feofilov (1961). *The physical basis of polarized emission*, Consultants Bureau, New York.
8. T. Förster (1948). Zwischenmolekulare Energiewanderung und Fluorescenz. *Ann. Phys.* **2**, 55–75.
9. G. Weber (1954). Dependence of the polarization of the fluorescence on the concentration. *Trans. Faraday Soc.* **50**, 552.
10. A. Kawski, P. Bojarski, A. Kubicki, and C. Bojarski (1991). On the mechanism of nonradiative electronic excitation energy transport in two-component systems concentration depolarization investigations. *J. Lumin.* **50**, 61–68.
11. J. Baumann and M. D. Fayer (1986). Excitation tranfer in disordered two-dimensional and anisotropic three-dimensional systems: Effects of spatial geometry on time-resolved observables. *J. Chem. Phys.* **85**, 4087.
12. J. Karolin and L. B.-Å. Johansson (1997). Donor–Donor Energy Migration (DDEM)—A new method for structure-function of proteins. *Trends Phys. Chem.* **6**, 171–185.
13. D. M. Jameson, J. C. Croney and P. D. J. Moens (2003). Fluorescence: Basic concepts, practical aspects, and some anecdotes. *Methods Enzymol.* **360**, 1–43.
14. L. B.-Å. Johansson, F. Bergström, P. Edman, I. V. Grechishnikova, and J. G. Molotkovsky (1996). Electronic energy migration and molecular rotation within bichromophoric macromolecules. Part 1. test of a model using bis(9-anthrylmethylphosphonate) bisteroid. *J. Chem. Soc., Faraday Trans.* **92**, 1563–1567.
15. L. B.-Å. Johansson, P. Edman, and P.-O. Westlund (1996). Energy migration and rotational motion within bichromophoric molecules. II. A derivation of the fluorescence anisotropy. *J. Chem. Phys.* **105**, 10896–10904.
16. M. L. Barcellona and E. Gratton (1996). Torsional dynamics and orientation of DNA–DAPI complexes. *Biochemistry* **35**, 321–333.
17. B. D. Hamman, A. V. Oleinikov, G. G. Jokhadze, R. R. Traut, and D. M. Jameson (1996). Dimer/monomer equilibrium and domain separations of Escherichia coli ribosomal protein L7/L12. *Biochemistry* **35**, 16680–16686.
18. M. P. Lillo, O. Canadas, R. E. Dale, and A. U. Acuna (2002). Location and properties of the taxol binding center in microtubules: A picosecond laser study with fluorescent taxoids. *Biochemistry* **41**, 12436–12449.
19. L. W. Runnels and S. F. Scarlata (1995). Theory and application of fluorescence homotransfer to melittin oligomerization. *Biophys. J.* **69**, 1569–1583.
20. P. Edman, P. Håkansson, P.-O. Westlund, and L. B.-Å. Johansson (2000). Extended Förster theory of donor-donor energy migration in bifluorophoric macromolecules. Part I. a new approach to quantitative analyses of the time-resolved fluorescence anisotropy. *Mol. Phys.* **98**, 1529–1537.
21. P. Edman, P.-O. Westlund, and L. B.-Å. Johansson (2000). On determining intramolecular distances from donor–donor energy migration (DDEM) within bifluorophoric macromolecules. *Phys. Chem. Chem. Phys.* **2**, 1789–1794.
22. P. Håkansson, M. Isaksson, P.-O. Westlund, and L. B.-Å. Johansson (2004). Extended Förster Theory for Determining Intraprotein Distances: The κ^2-Dynamics and Fluorophore Reorientation, *J. Phy. Chem.*, In press.
23. G. A. Silverman, P. I. Bird, R. W. Carrell, F. C. Church, P. B. Coughlin, P. G. Gettins, J. A. Irving, D. A. Lomas, C. J. Luke, R. W. Moyer, P. A. Pemberton, E. Remold-O'Donnell, G. S. Salvesen, J. Travis, and J. C. Whisstock (2001). The serpins are an expanding superfamily of structurally similar but functionally diverse proteins. Evolution, mechanism of inhibition, novel functions, and a revised nomenclature. *J. Biol. Chem.* **276**, 33293–33296.
24. M. Fa, F. Bergström, P. Hägglöf, M. Wilczynska, L. B.-Å. Johansson, and T. Ny (2000). The structure of a serpin–protease complex revealed by intramolecular distance measurements using donor-donor energy migration and mapping of interaction sites. *Structure* **8**, 397–405.
25. P. Hägglöf, F. Bergström, M. Wilczynska, L. B.-Å. Johansson, and T. Ny (2004). The reactive-centre loop of active PAI-1 is folded close to the protein core and can be partially inserted. *J. Mol. Biol.* **335**, 823–832.
26. S. Scarlata, L. S. Ehrlich, and C. A. Carter (1998). Membrane-induced alterations in HIV-1 Gag and matrix protein–protein interactions. *J. Mol. Biol.* **277**, 161–169.
27. N. C. Santos, M. Prieto, and M. Castanho (1998). Interaction of the major epitope region of HIV protein gp41 with membrane model systems. A fluorescence spectroscopy study. *Biochemistry* **37**, 8674–8682.
28. P. I. H. Bastiaens, A. Van Hoek, J. A. E. Benen, J. C. Brochon, and A. J. W. G. Visser (1992). Conformational dynamics and intersubunit energy transfer in wild-type and mutant lipoamide dehydrogenase from Azotobacter vinelandii. A multidimensional time-resolved polarized fluorescence study. *Biophys. J.* **63**, 839–853.
29. F. Tanaka and N. Mataga (1979). Theory of time-dependent photoselection in interacting fixed media. *Photochem. Photobiol.* **29**, 1091–1097.
30. Y. R. Kim, P. Share, M. Pereira, M. Sarisky, and R. M. Hochstrasser (1989). Direct measurements of energy transfer between identical chromophores in solution. *J. Chem. Phys.* **91**, 7557–7562.
31. J. M. Mullaney, R. B. Thompson, Z. Gryczynski, and L. W. Black (2000). Green fluorescent protein as a probe of rotational mobility within bacteriophage T4, *J. Virol. Methods* **88**, 35–40.
32. I. Gautier, M. Tramier, C. Durieux, J. Coppey, R. B. Pansu, J. C. Nicolas, K. Kemnitz, and M. Coppey-Moisan (2001). Homo-FRET microscopy in living cells to measure monomer-dimer transition of GFP-tagged proteins. *Biophys. J.* **80**, 3000–3008.
33. A. H. A. Clayton, Q. S. Hanley, D. J. Arndt-Jovin, V. Subramaniam, and T.M. Jovin (2002). Dynamic fluorescence anisotropy imaging microscopy in the frequency domain (rFLIM). *Biophys. J.* **83**, 1631–1649.
34. J. V. Rocheleau, M. Edidin, and D. W. Piston (2003). Intrasequence GFP in class I MHC molecules, a rigid probe for fluorescence anisotropy measurements of the membrane environment. *Biophys, J.* **84**, 4078–4086.
35. G. H. Patterson, D. W. Piston, and B. G. Barisas (2000). Förster distances between green fluorescent protein pairs. *Anal. Biochem.* **284**, 438–440.
36. M. Tramier, T. Piolot, I. Gautier, V. Mignotte, J. Coppey, K. Kemnitz, C. Durieux, and M. Coppey-Moisan (2003). Homo-FRET versus hetero-FRET to probe homodimers in living cells. *Methods Enzymol.* **360**, 580–597.
37. J.-C. Rochet and J. Lansbury (2000). Amyloid fibrillogenesis: Themes and variations. *Curr. Opin. Struct. Biol.* **10**, 60–68.
38. C. M. Dobson (2003). Protein folding and misfolding. *Nature* **426**, 884–890.
39. L. Erijman and G. Weber (1991). Oligomeric protein associations—transition from stochastic to deterministic equilibrium. *Biochemistry* **30**, 1595–1599.
40. L. Erijman and G. Weber (1993). Use of sensitized fluorescence for the study of the exchange of subunits in protein aggregates. *Photochem. Photobiol.* **57**, 411–415.
41. S. M. Blackman, D. W. Piston, and A. H. Beth (1998). Oligomeric state of human erythrocyte band 3 measured by fluorescence resonance energy homotransfer. *Biophys. J.* **75**, 1117–1130.
42. J. Howard and A. A. Hyman (2003). Dynamics and mechanics of the microtubule plus end. *Nature* **422**, 753–758.
43. R. Varma and S. Mayor (1998). GPI-anchored proteins are organized in submicron domains at the cell surface. *Nature* **394**, 798–801.

44. C. E. MacPhee, G. J. Howlett, W. H. Sawyer, and A. H. A. Clayton (1999). Helix–helix association of a lipid-bound amphipathic alpha-helix derived from apolipoprotein C-II. *Biochemistry* **38**, 10878–10884.
45. M. J. E. Prieto, M. Castanho, A. Coutinho, A. Ortiz, F. J. Aranda, and J. C. Gomezfernandez (1994). Fluorescence study of a derivatized diacylglycerol incorporated in model membranes. *Chem. Phys. Lipids* **69**, 75–85.
46. I. Mikhalyov, S.-T. Bogen, and L. B.-Å. Johansson (2001). Donor–Donor Energy Migration (DDEM) as a tool for studying aggregation in lipid phases. *Spectrochim. Acta Part A* **57**, 1839–1845.
47. S.-T. Bogen, G. de Korte-Kool, G. Lindblom, and L. B.-Å. Johansson (1999). Aggregation of an α- helical transmembrane peptide in lipid phases, studied by time resolved fluorescence spectroscopy. *J. Phys. Chem. B* **103**, 8344–8352.
48. M. N. Berberan-Santos and B. Valeur (1991). Fluorescence depolarization by electronic energy transfer in donor–acceptor pairs of like and unlike chromophores. *J. Chem. Phys.* **95**, 8048–8055.
49. M. N. Berberan-Santos, P. Choppinet, A. Fedorov, L. Jullien, and B. Valeur (1999). Multichromophoric cyclodextrins. 6. Investigation of excitation energy hopping by Monte-Carlo simulations and time-resolved fluorescence anisotropy. *J. Am. Chem. Soc.* **121**, 2526–2533.
50. S. Blonski and K. Sienicki (1991). Energy-transfer and migration in Langmuir-Blodgett-Films - Monte-Carlo Simulations. *J. Phys. Chem.* **95**, 7353–7357.
51. P. Bojarski, A. Kaminska, L. Kulak, and M. Sadownik (2003). Excitation energy migration in uniaxially oriented polymer films. *Chem. Phys. Lett.* **375**, 547–552.
52. L. B.-Å. Johansson, S. Engström, and M. Lindberg (1992). Electronic energy transfer in anisotropic systems. III. Monte Carlo simulations of energy migration in membranes. *J. Chem. Phys.* **96**, 3844–3856.
53. P. G. Wu, B. S. Fujimoto, L. Song, and J. M. Schurr (1991). Effect of ethidium on the torsion constants of linear and supercoiled DNAs. *Biophys. J.* **41**, 217–236.
54. S. Engström, M. Lindberg, and L. B.-Å. Johansson (1992). Fluorescence anisotropy of rotating molecules in presence of energy migration. *J. Chem. Phys.* **96**, 7528–7534.
55. P. Håkansson, L. Persson, and P.-O. Westlund (2002). Ito diffusions on hyper surfaces with application to the Schwatz-P-surface and nuclear magnetic resonance theory. *J. Chem. Phys.* **117**, 8634–8643.
56. W. Maier and A. Saupe (1959). Eine einfache molekular-statistische Theorie der nematischen kristallinflüssigen Phase. *Z. Naturforsch. A* **14**, 882–889.
57. F. N. Chowdhury, Z. S. Kolber, and M. D. Barkley (1991). Monte Carlo convolution method for simulation and analysis of fluorescence decay data. *Rev. Sci. Intrum.* **62**, 47.
58. D. V. O'Connor and D. Phillips (1984). Time-correlated Single Photon Counting, Academic Press, London.
59. S. Kalinin and L. B.-Å. Johansson (2004). Energy migration and transfer rates are invariant to modelling the fluorescence relaxation by discrete and continuous distributions of lifetimes. *J. Phys. Chem. B* **108**, 3092–3097.
60. S. V. Kalinin, J. G. Molotkovsky, and L. B.-Å. Johansson (2002). Partial Donor–Donor energy migration (PDDEM) as a fluorescence spectroscopic tool of measuring distances in biomacromolecules. *Spectrochim. Acta Part A* **58**, 1087–1097.
61. P. Woolley, K. G. Steinhauser, and B. Epe (1987). Forster-type energy-transfer–simultaneous forward and reverse transfer between unlike fluorophores. *Biophys. Chem.* **26**, 367–374.
62. K. Engelborghs (2001). The analysis of time resolved protein fluorescence in multi-tryptophan proteins. *Spectrochim. Acta Part A* **57**, 2255–2270.
63. K. Willaert, R., Loewenthal, J. Sancho, M. Froeyen, A. Fersht, and Y. Engleborghs (1992). Determination of the excited state lifetimes of the tryptophan residues in barnase, via multifrequency phase fluorimetry of tryptophan mutants. *Biochemistry* **31**, 711–716.
64. S. Verheyden, A. Sillen, A. Gils, P. J. Declerck, and Y. Engelborghs (2003). Tryptophan properties in fluorescence and functional stability of plasminogen activator inhibitor 1. *Biophys. J.* **85**, 501–510.
65. M. Isaksson, S. Kalinin, S. Lobov, S. Wang, T. Ny and L. B.-Å. Johansson (2004). Distance measurements in proteins by fluorescence using Partial Donor–Donor Energy Migration (PDDEM). *Phys. Chem. Chem. Phys.* **6**, 3001–3008.
66. S. Kalinin, J. G. Molotkovsky, and L. B.-Å. Johansson (2003). Distance measurements using Partial Donor–Donor Energy Migration (PDDEM) within pairs of fluorescent groups in lipid bilayers. *J. Phys. Chem. B* **107**, 3318–3324.
67. P. Bojarski and A. Jankowicz (1999). Excitation energy transport between the ionic forms of rhodamine B in viscous solutions. *J. Lumin.* **81**, 21–31.
68. R. P. Haugland (2002). *Handbook of Fluorescent Probes and Research Products*, 9th ed., Molecular Probes.
69. Z. W. Zhang, B. A. C. Smith, L. Wang, A. Brock, C. Cho, and P. G. Schultz (2003). A new strategy for the site-specific modification of proteins in vivo. *Biochemistry* **42**, 6735–6746.
70. L. Wang, A. Brock, B. Herberich, and P. G. Schultz (2001). Expanding the genetic code of Escherichia coli. *Science* **292**, 498–500.
71. B. E. Cohen, T. B. McAnaney, E. S. Park, Y. N. Jan, S. G. Boxer, and L. Y. Jan (2002). Probing protein electrostatics with a synthetic fluorescent amino acid. *Science* **296**, 1700–1703.
72. M. Taki, T. Hohsaka, H. Murakami, K. Taira, and M. Sisido (2001). A non-natural amino acid for efficient incorporation into proteins as a sensitive fluorescent probe. *FEBS Lett.* **507**, 35–38.
73. G. Turcatti, K. Nemeth, M. D. Edgerton, U. Meseth, F. Talabot, M. Peitsch, J. Knowles, H. Vogel, and A. Chollet (1996). Probing the structure and function of the tachykinin neurokinin-2 receptor through biosynthetic incorporation of fluorescent amino acids at specific sites. *J. Biol Chem.* **271**, 19991–19998.
74. V. W. Cornish, D. R. Benson, C. A. Altenbach, K. Hideg, W. L. Hubbell, and P. G. Schultz (1994). Site-specific incorporation of biophysical probes into proteins. *Proc. Natl. Acad. Sci. USA* **91**, 2910–2914.